Progress Report, 2005, Southern California Earthquake Center

Dynamics of Rupture Propagation with Fault Branches, Stepovers, and Damaged Border zones

James R. Rice (PI) and Renata Dmowska (Co-PI), Harvard University, Cambridge, MA 02138
20 November 2005

Recent reports related to theme of this project:

Bhat, H. S., R. Dmowska, J. R. Rice and N. Kame (2004), "Dynamic slip transfer from the Denali to Totschunda Faults, Alaska: Testing theory for fault branching", *Bulletin of the Seismological Society of America,* **94**(6B), pp. S202-S213. http://esag.harvard.edu/dmowska/BhatDmRiKa_Denali_BSSA04.pdf

Bhat, H. S., R. Dmowska, G. King, Y. Klinger, and J. R. Rice (2005), "Supershear slip pulse and off-fault damage", *Eos Trans. AGU, 86(52),* Fall Meet. Suppl., Abstract S34A-06.

Bhat, H. S., R. Dmowska, G. King, Y. Klinger, and J. R. Rice (2005), "Off-fault damage patterns due to supershear ruptures with application to the 2001 Mw 8.1 Kokoxili (Kunlun) Tibet earthquake", manuscript in semifinal draft, to be submiited to *Journal of Geophysical Research*. http://esag.harvard.edu/rice/BhatDmKiKlRi_supershear_10Sep05.pdf

Fliss, S., H. S. Bhat, R. Dmowska and J. R. Rice (2005), "Fault branching and rupture directivity", *Journal of Geophysical Research,* 110, B06312, doi:10.1029/2004JB003368, 22 pages. http://esag.harvard.edu/dmowska/FlissBhatDmRi_JGR05.pdf

Rice, J. R., C. G. Sammis and R. Parsons (2005), "Off-fault secondary failure induced by a dynamic slip-pulse", *Bulletin of the Seismological Society of America*, 95(1), pp. 109–134, doi: 10.1785/0120030166. http://esag.harvard.edu/rice/211_RiceSammisPars_BSSA05.pdf

Templeton, E. L., A. Baudet, H. S. Bhat, R. Dmowska, J. R. Rice, A. J. Rosakis, and C. E. Rousseau (2005), "Finite element simulations of dynamic shear rupture experiments and path selection along ranched faults", *Eos Trans. AGU, 86(52),* Fall Meet. Suppl., Abstract S43 A-1066.

Xia, K., A. J. Rosakis, H. Kanamori and J. R. Rice (2005), "Laboratory earthquakes along inhomogeneous faults: Directionality and supershear", *Science*, 308 (5722), pp. 681-684. http://esag.harvard.edu/rice/ 215_XiaRosKanRi_bimat_Sci05.pdf

Progress

Role of minor branch structures in rupture dynamics. We have continued our studies on the role of short fault branches as a source of seismic complexities and generation of high frequency content of the ground motion (Figures 1 and 2). Earlier works on the latter have shown that abrupt changes in rupture velocity, due to an asperity or as in this case by the introduction of a short branch, can lead to the generation of such high frequency content. We simulate the propagation using a 2D elastodynamic BIE formulation of Kame et al. [*JGR*, 2003] incorporating a slip-weakening Coulomb friction failure criterion. We parameterize the problem with the inclination Ψ of maximum principal compressive stress with the main fault, inclination ϕ of the branch, rupture velocity v_r at the branching junction, and the length of the branch.

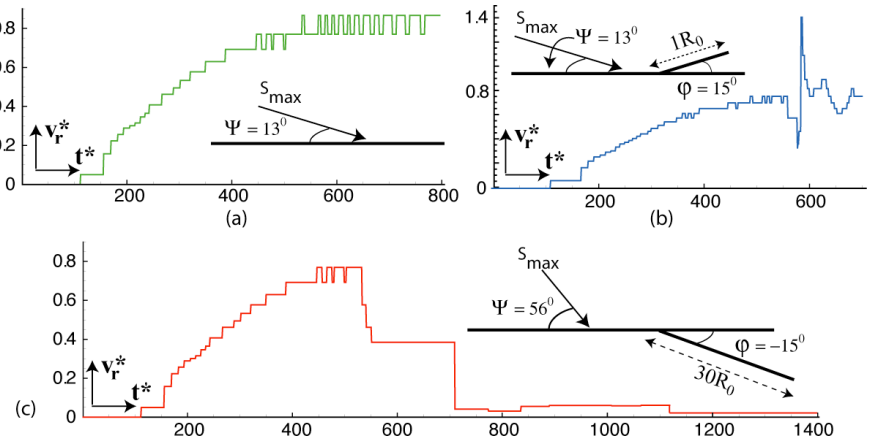

Figure 1 [Bhat et al., in progress, 2005]: Results are from BIE numerical simulations, assuming slip-weakening of a Coulomb friction coefficient, the same weakening for all fault segments. Right-lateral rupture is nucleated and propagates to the right on a horizontal fault, with different principal compressive pre-stress directions (at angles Ψ), and with (a) no branch, (b) a short finite branch to the compressional side, and (c) a much longer but also finite branch to the extensional side. Ruptures must stop at branch ends. Nondimensional rupture speed $v_r^* = v_r / c_s$ is shown as a function of nondimensional time t^*; $v_r = 0.80 c_s$ when approaching the branch junctions. In case (b), a burst of supershear rupture occurs after branch interaction and a brief slowdown. Instead, in case (c), the presence of the branch arrests propagation of the rupture. The length scale R_0 is the slip-weakening zone length, based on the assumed slip-weakening relation, for low speed crack propagation. Rice et al. [2005] estimate it, from seismic slip inversion results, to be typically a few tens of meters at mid-seismogenic zone depths, and to scale inversely with the effective normal stress on the fault. Such branch interactions imprint the fault with a locally nonuniform residual stress state after rupture, which may contribute to future complexities.

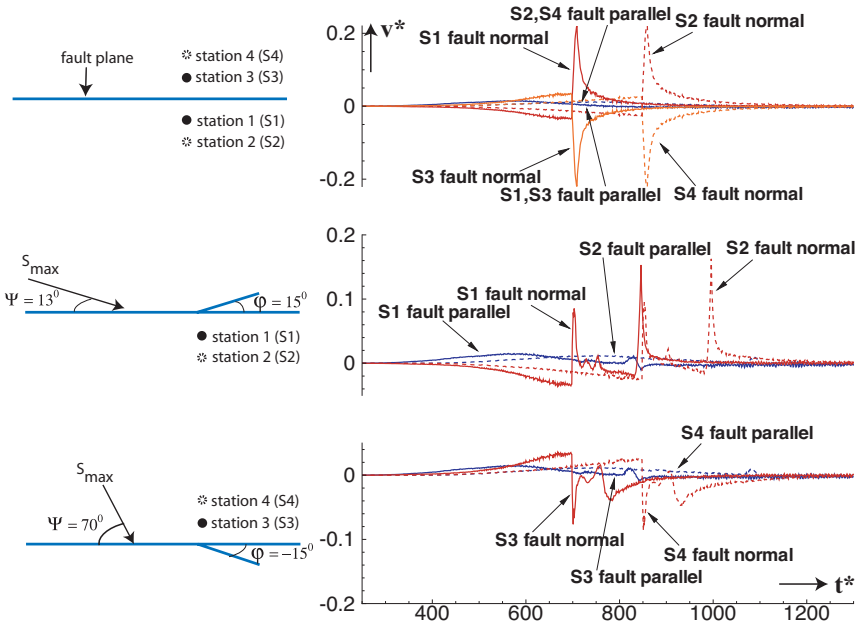

Figure 2 [Bhat et al., in progress, 2005]: Normalized particle velocities, v*, (unfiltered fault parallel and fault normal) predicted at near-fault positions, offset in normal direction by distances $\pm 15 R_0$ and $\pm 30 R_0$. The length of the branches in the last two cases is R_0. $v_r = 0.80 c_s$ when approaching the branch junctions.

We show, Figure 1, some representative cases where the introduction of a very short branch, of length equal to the size R_0 of the slip-weakening zone at low rupture velocity, can significantly perturb the rupture velocity on the main fault. Rice et al. [*BSSA*, 2005] estimate this length to be few tens of meters, by fitting parameters of their propagating slip pulse model to results of seismic slip inversions. That is quite small compared to the length of the faults. Such features are encountered in natural events, like the 1992 Landers rupture. Figure 1b shows a brief transition of the rupture on the main fault to the supershear regime as the rupture on the branch radiates significant stress changes when stopped suddenly. Figure 1c shows a mechanism for the complete arrest of rupture on the main fault via the introduction of a long branch, of length $30R_0$.

Off-fault stressing due to steady state supershear slip pulse propagation. In analyzing the off-fault damage induced by supershear rupture, and hence possibly identifying unique features associated with this speed regime, Bhat et al. [2005] have studied a 2D steadily propagating slip pulse in an ideally elastic material, like in the Rice et al. [2005] pulse model, solved for supershear by Dunham and Archuleta [BSSA, 2005]. In the supershear range the high stresses radiate out to infinity along shear wave Mach lines. In a realistic 3D setting they are expected to radiate out from the fault over distances which may be comparable to the depth of the seismogenic zone. Regions over which elastically predicted stress levels are large enough to induce Mohr-Coulomb failure in the surroundings can then, in certain circumstances, extend out to several kilometers from the fault, versus just the tens to hundreds of meters that we have estimated in representative sub-Rayleigh cases by fitting model parameters to results of seismic slip inversions [Rice et al., 2005]. See Figure 3.

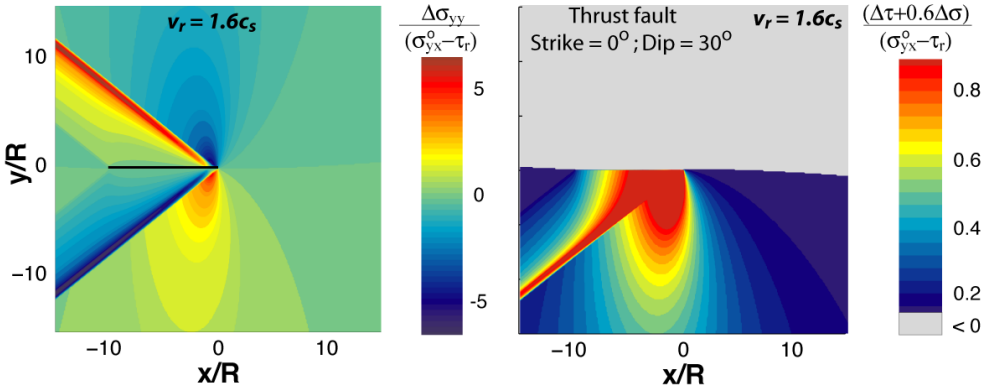

Figure 3: Supershear version [Bhat et al., 2005] of 2D steady state slip pulse model. Contour plot at left shows fault-normal stress changes normalized by dynamic stress drop, for $v_r = 1.6c_s$. Note that very large stress changes, in this case of magnitude ~3 times the dynamic stress drop, are radiated far from the fault along the Mach fronts. Changes of equal magnitude but reversed sign are radiated in the fault-parallel component far from the fault. Results for $R/L = 0.10$ where R and L are the size of the slip-weakening zone and the length of the slip pulse respectively. Contour plot on the right shows the change in Coulomb stress, normalized by dynamic stress drop, induced by a supershear slip pulse on thrust faults striking parallel to the slip pulse and dipping at 30^0. Notice the radiation of large stress changes along the Mach fronts.

Correlation with and simulation of laboratory rupture dynamics. We are collaborating with Ares Rosakis of Caltech and co-workers on laboratory study of fracture dynamics. Last year we reported on Elizabeth Templeton's simulations of the published results of Rousseau and Rosakis [*JGR,* 2003] on the impact-induced shear fracture along kinked failure paths in brittle

photoelastic materials. More recently, Rosakis and Rousseau have refocused their efforts with this type of impact experiment to specimens with precut surfaces to simulate a main fault with a branch fault running off of it. We have simulated slip-weakening rupture for such branch cases using the ABAQUS/Explicit dynamic finite element program, with a slip weakening constitutive response written via a user-defined frictional constitutive option, VFRIC, which is essentially implemented as a split node procedure.

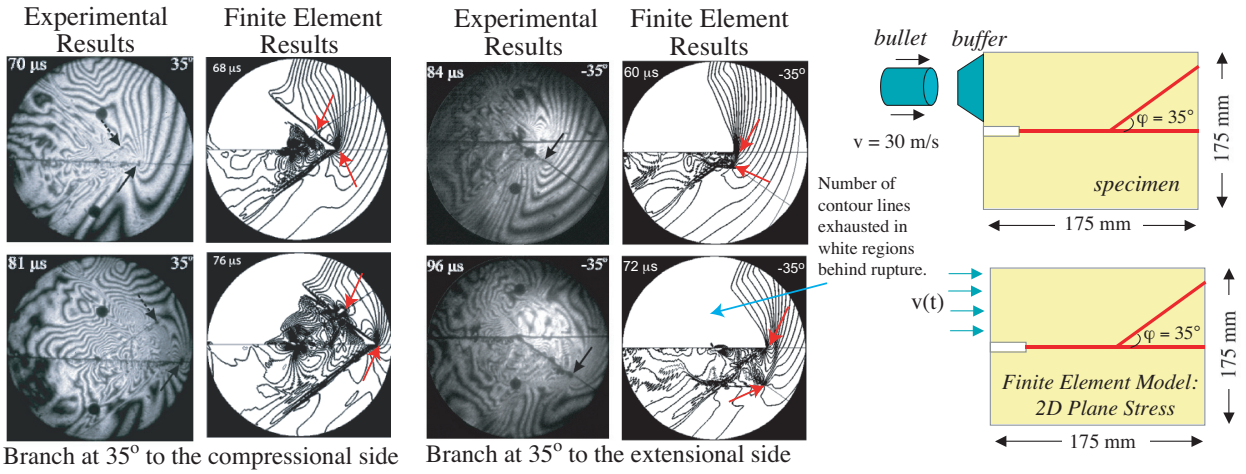

Figure 4: Finite element simulation [Templeton et al., 2005] of Rousseau and Rosakis 2004-2005 branching experiments. A photoelastic Homalite plate with an initial weakened, branched path is hit by a steel bullet traveling at 30 m/s. The notch below the buffer prevents immediate transmission of stress waves to the bottom half, allowing a mode-II rupture to initiate along the weakened path.

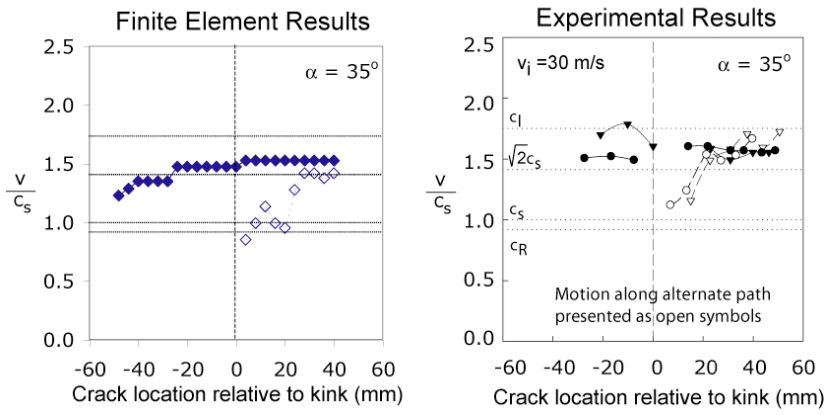

Figure 5: Rupture velocities from a Rousseau-Rosakis 2004-2005 branching experiment at right; dynamic rupture simulation [Templeton et al., 2005] at left. Solid symbols show rupture speed on the main (horizontal) fault. Open symbols show speed on the branch fault.

Results are shown for two branched specimen cases, a branch at 35° from the main fault to the compressive side, and at 35° to the extensional side. As in our previous studies of kinked faults, impact is represented in the finite element simulations as an imposed velocity history at the impact faces. Figure 4 shows a preliminary comparison of intersonic simulations with intersonic experimental isochromatic lines (lines of constant difference between the in-plane principal stresses), for the two cases. Rupture proceeds along the main fault at an intersonic

speed, approaching the P-wave speed, before reaching the branch junction. The Mach front structure can be seen in both the simulations and the experiments. When the rupture reaches the branch junction, a new rupture begins along the branch with a velocity near the S-wave speed, as shown in Figure 5, and ultimately propagates at a speed close to the P-wave speed. The rupture along the branched fault appears to be driven by the shock fronts from the rupture along the main fault. In order to optimize the fit to the experimental results, we are studying the influence on simulation results of assumptions concerning slip weakening in both (1) the cohesive part of the strength (a part independent of normal stress) and (2) the friction coefficient for the frictional part of strength that is proportional to normal stress.

Interaction of off-fault inelastic deformation with rupture dynamics. We have also focused on adapting the finite element procedure to a wide range of problems in rupture dynamics, including the interaction of off-fault inelasticity with rupture propagation; see the new proposal on that topic. The ABAQUS/Explicit program includes options for modeling continuum elastic-plastic deformation within elements by a Drucker-Prager type of granular medium plasticity (very similar to Mohr-Coulomb plasticity for plane strain problems), among other options, and also by user-defined tensorial constitutive models which can be entered by its VUMAT option. We have begun implementing the Drucker-Prager plasticity model for a simple planar fault in an elastic-plastic material, subject to uniform prestress at a level producing sub-Rayleigh rupture propagation speeds. Figure 6 compares two cases that would have had identical rupture response if we had assumed purely elastic material off the fault plane. The size of the plastic zone that develops, and the magnitudes of plastic strain produced, depend significantly on the direction of maximum compressive stress, Ψ. When $\Psi > 45°$, a broad zone of plastic strain develops on the extensional side of the fault, but when $\Psi < 15°$, a narrow zone of plastic strain develops on both sides of the fault.

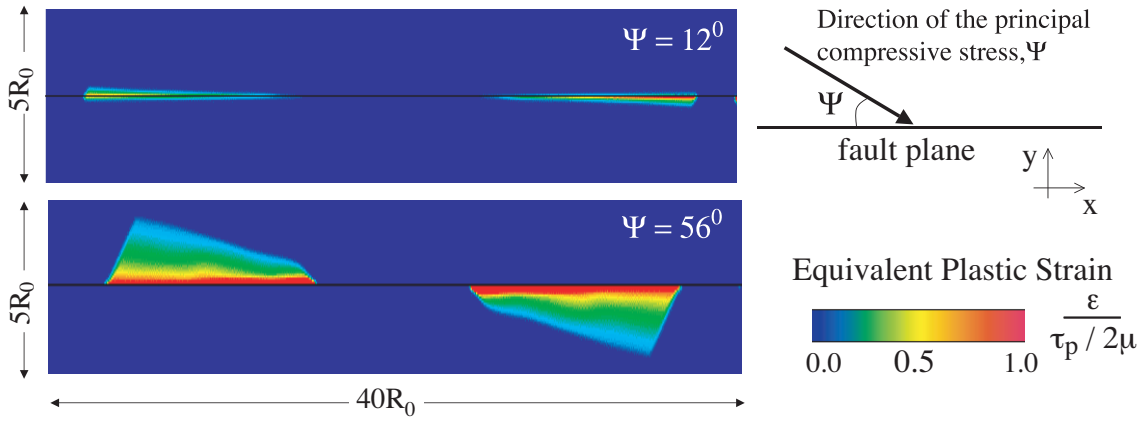

Figure 6: Off-fault plastic strain. [E. Templeton and H. Bhat, 2005]. Here ε is the equivalent plastic shear strain based on the second invariant of the plastic strain tensor; $\tau_p/2\mu$ is the elastic shear strain corresponding to the peak shear strength (τ_p) along the fault. Both cases have the seismic ratio S = 2, and the initial stress tensors are comparable fractions of yield. The $\Psi = 12°$ case leads to results only modestly different from those for an elastic material, but in the $\Psi = 56°$ case rupture is more difficult to nucleate and propagation is much slower (see the final figure in our recent proposal). The maximum plastic equivalent shear strain in the $\Psi = 56°$ case is comparable to the elastic shear strain at peak shear strength.